

Figure. 4.13: Typical XRD patterns of GO irradiated by sunlight and artificial light for different durations.

4.7.4.4 ATR-FTIR spectroscopy investigations

Figure 4.14 depicts ATR-FTIR patterns of GO irradiated by sunlight or artificial light sources with different filters for different durations. From the ATR-FTIR spectra, we see that the intensity of the carbonyl stretching band (1610cm^{-1}) decreases substantially after ~ 2 hours irradiation (**Figure 4. 14**).

Similarly, the intensities of other bands due to other oxygen containing functional groups also decrease after the prolonged sunlight/artificial light sources with different filters irradiation. At 1620 cm^{-1} (skeletal vibrations from un-oxidized graphitic domains), at 1220 cm^{-1} (C-OH stretching vibrations), at 1060 cm^{-1} (C-O stretching vibrations), and stretching vibrations from C=O at 1720 cm^{-1} due to the remaining of carboxyl groups and the vibration modes of epoxide (C-O-C) at ($1230\text{-}1320\text{ cm}^{-1}$, asymmetric stretching at 850 cm^{-1} , bending motion).

WESTERN CAPE

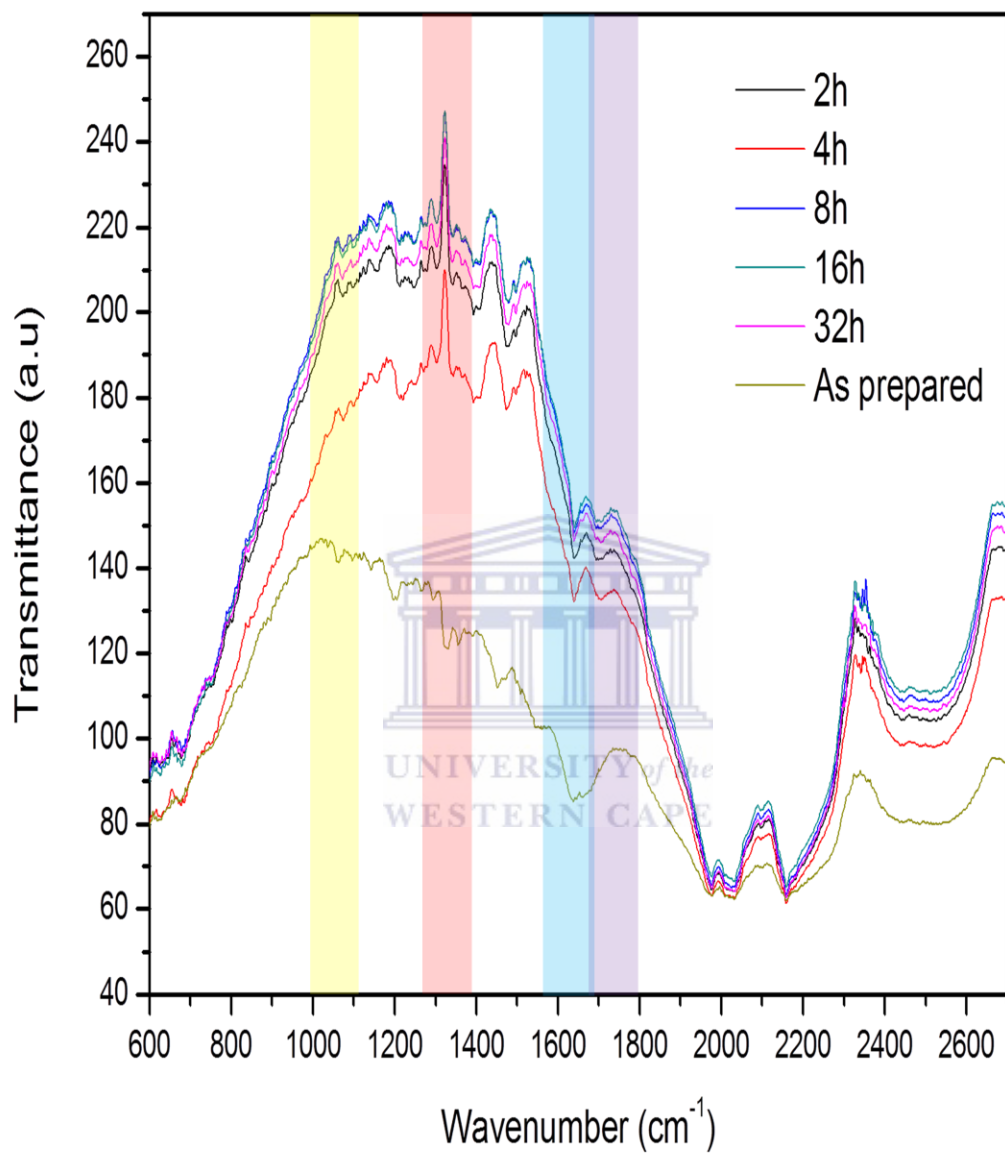


Figure. 4.14: Typical ATR-FTIR patterns of GO irradiated by sunlight and artificial light for different durations.

4.7.4.5 UV-Vis Absorbance spectroscopy investigations

The color change of the graphene oxide from brownish yellow to black is a clear evidence of the occurrence of reduction via sunlight or artificial light irradiation. The dynamic of photo-reduction by all radiations can be monitored easily with UV-UVIS absorbance spectroscopy. Indeed, the GO absorbance spectrum is known by the presence of three principal peaks, the main absorbance peak attributed to the $\pi \rightarrow \pi^*$ transitions of C-C occurs at around 225 nm, the broad absorption spectra extended up to 450 nm indicating a well-defined band-edge in the UV-VIS energy range and a shoulder around 320nm may be attributed to the $\pi \rightarrow \pi^*$ transitions of C-O. The Transformation of GO in our samples, reduced by sunlight as well as by artificial filtered light, is confirmed by the slow disappearance of C-C band centered at around 225 nm and its shifting to 260nm upon exposition time most likely due to the decrease in the concentration of carboxyl groups shown in Figure 4.15 indicating that the electronic conjugation within the reduced graphene sheets was revived upon reduction of graphene oxide.

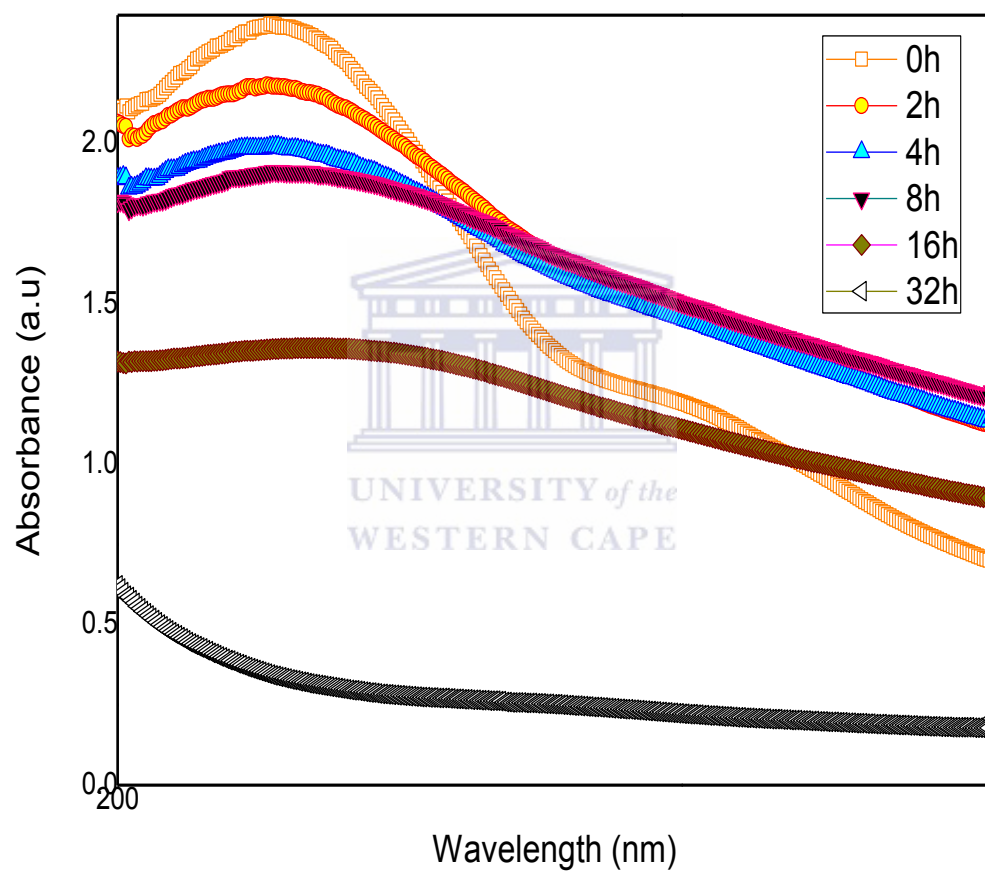
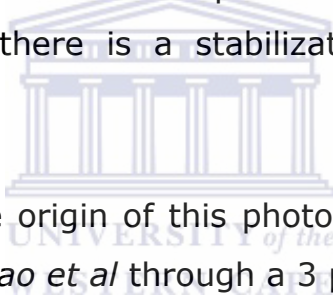
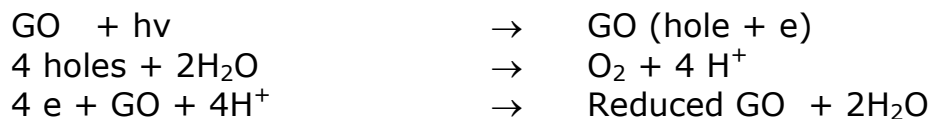


Figure. 4.15: Typical UV-Vis absorbance spectra of GO irradiated by sunlight for different durations.

Figures 4.16-19. depict the UV-Vis absorbance spectra of the various photo-reduced GO nano-solutions under both white light and filtered artificial light sources for various exposure time. It can be observed that the red filtered irradiated solution for various exposure time have roughly similar trend as the as prepared solution even after 16h of irradiation. In opposite, one could distinguish the significant effects of the yellow and blue filtered artificial radiations in addition to the well established white irradiation photo-reduction phenomena. Indeed, as it is illustrated in Figure 4.16-19, the absorbance profiles of these radiations have similar trends. In all corresponding spectra, the specific absorbance in the UV-VIS range quasi-disappear and are smoothed on a wide spectral range. This behavior seems to start at about the threshold exposure time of about 4. After 8h of irradiation, it seems that there is a stabilization of the photo-reduction process.



The process which is at the origin of this photo-induced chemical reduction sustain the explanation of *Rao et al* through a 3 phases mechanism.



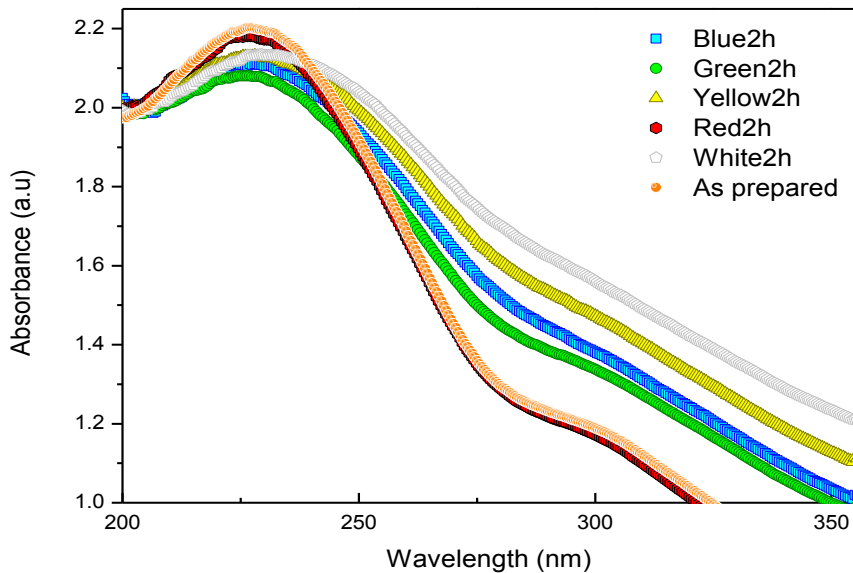


Figure. 4.16: The various UV-Vis absorbance spectra of GO irradiated by different filtered artificial light for 2h.

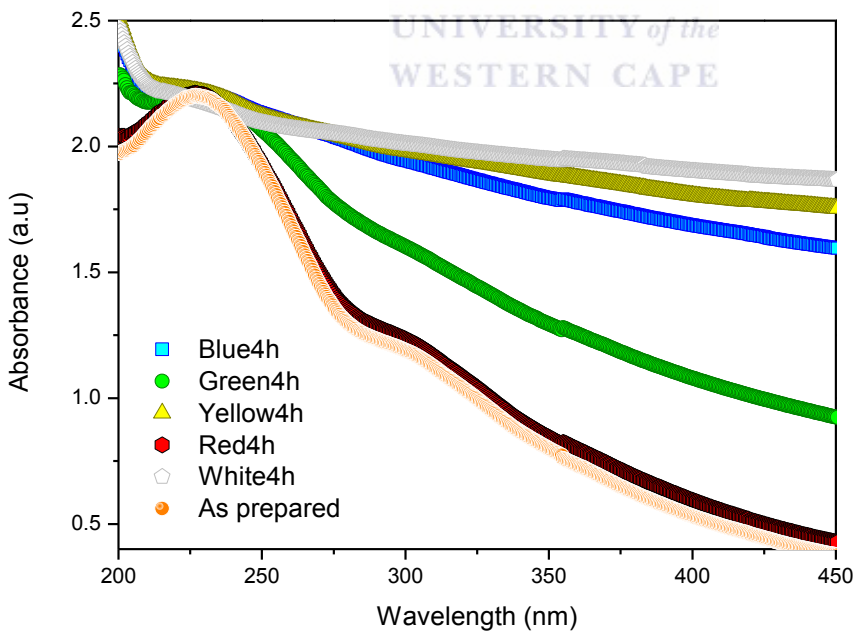


Figure. 4.17: The various UV-VIS absorbance spectra of GO irradiated by different filtered artificial lights for 4h.

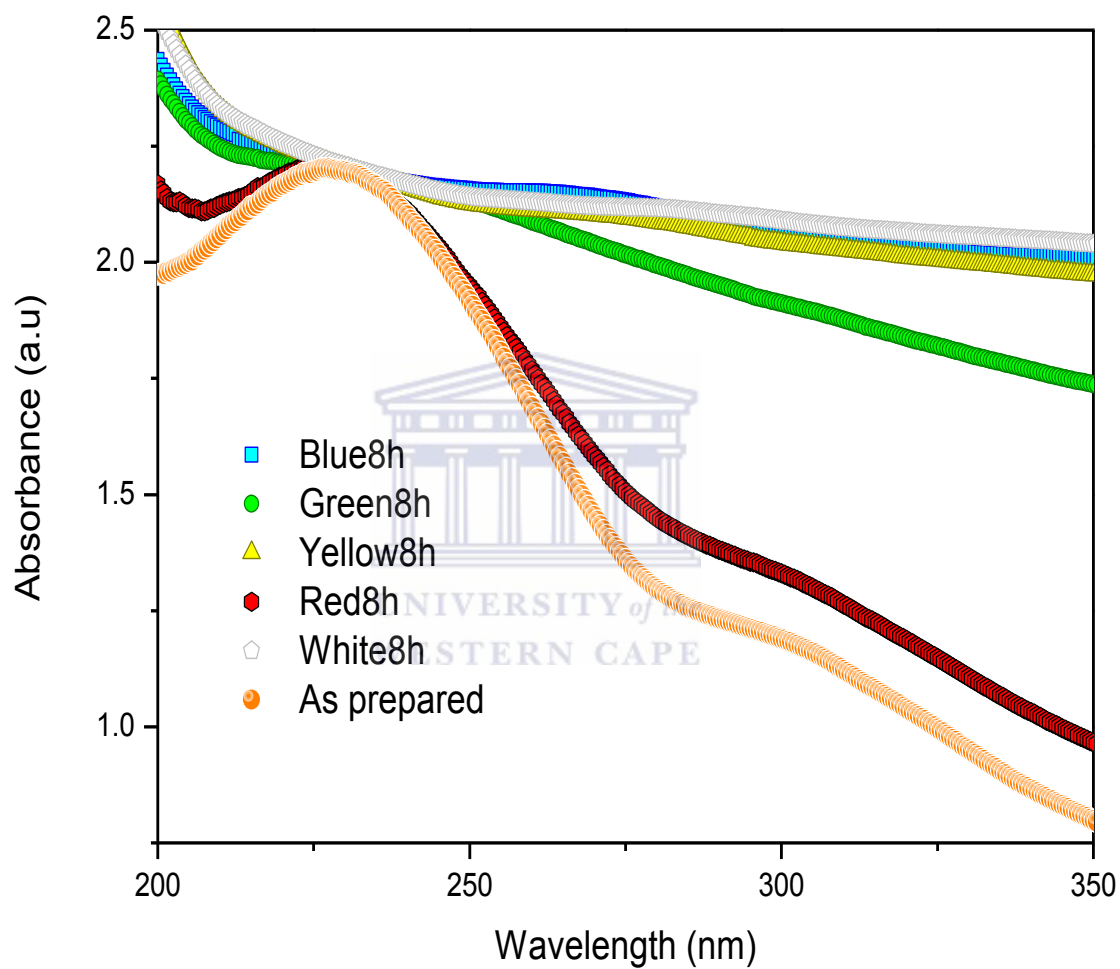


Figure. 4.18: The various UV-Vis absorbance spectra of GO irradiated by different filtered artificial lights for 8h.

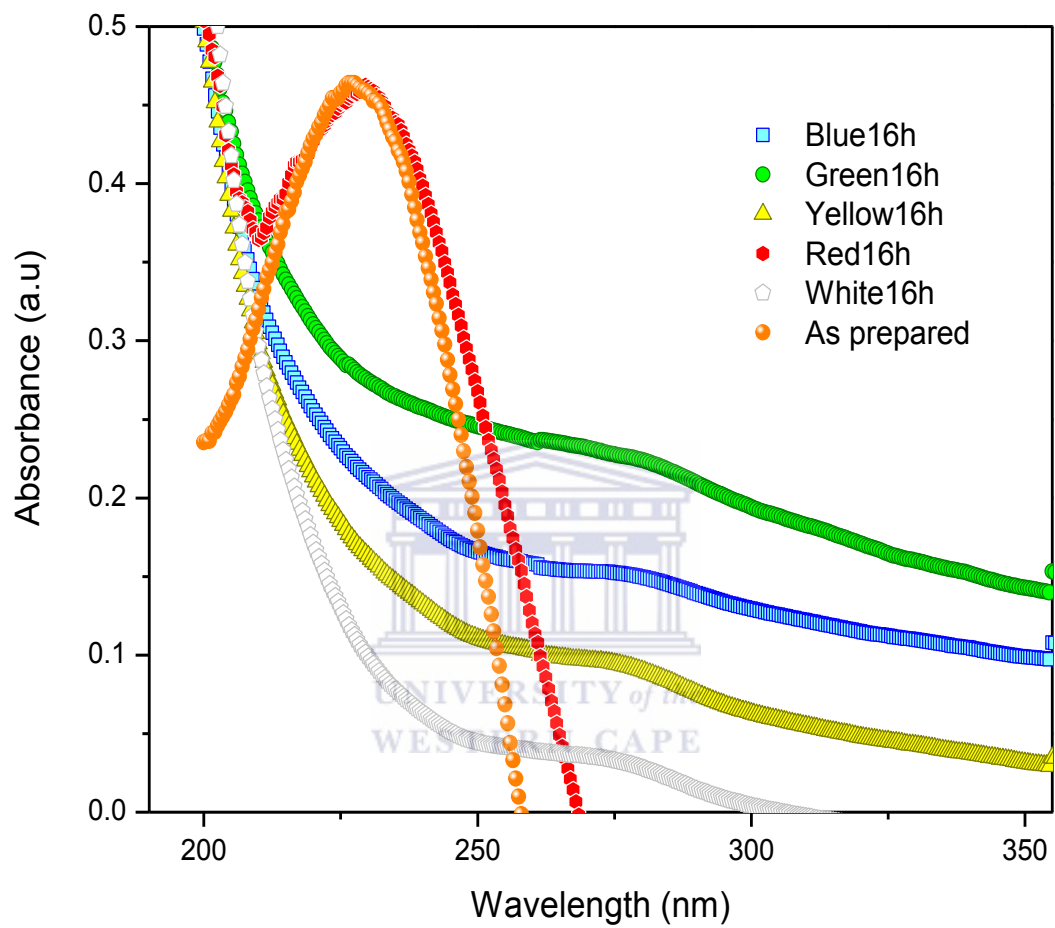


Figure. 4.19: The various UV-Vis absorbance spectra of GO irradiated by different filtered artificial lights for 16h.

4.8 References

- [1]. Hummers W.S., Offeman R.E., Preparation of graphitic oxide. *J Am Chem Soc* 1958;80:1339.
- [2]. Chengyi H., Qinghong Z., Meifang Z., Yaogang L., Hongzhi W., One-step synthesis of magnetically-functionalized reduced graphite sheets and their use in hydrogels. *Carbon* DOI:10.1016/j.carbon.2010.08.040.
- [3]. Xu C.H., Lee Y. H., Kim S. G., Rinzler A. G., *J. Am. Chem. Soc.* 2008, 130, 5856–5857. 46.
- [4]. Li D., Muller M. B., Gilje S., Kaner R. B., Wallace G. G., Processable aqueous of graphene nanosheets, *Nature Nanotechnology*, 3(2), 2008, 101-105
- [5]. Stankovich S., Dikin D. A., Piner R. D., Kohlhaas K. A., Kleinhammes A. Jia Y., Wu Y., Nguyen S. T., Ruoff R.S., Synthesis of Graphene-Based Nanosheets *via* Chemical Reduction of Exfoliated Graphite Oxide. *Carbon* 2007, 45, 1558–1565.
- [6]. Xu Y., Bai H, Lu G., Li C., Shi G., Flexible graphene films via the filtration of water-soluble noncovalent functionalized graphene sheets. *J. Am. Chem. Soc.* 2008, 130, 5856–5857.
- [7]. Ruoff R., *Nat. Nano* 2008, 3 (1), 10–11.
- [8]. Lerf A., He H., Forster M., Klinowski J., *J. Phys. Chem. B* 1998, 102 (23), 4477–4482.
- [9]. Fasolino A., Los J. H., Katsnelson M. I., Intrinsic ripples in graphene. *Nature Materials* 6, 858-861 (2007)
- [10]. Nethravathi C., Viswanath B., Shivakumara C., Mahadevaiah N., Rajamathi M., *Carbon* 2008, 46, 1773.

- [11]. Bourlinos A.B., Gournis D., Petridis D., Szabo T., Szeri A., Dekany I. *Langmuir* 2003, 19, 6050
- [12]. Ferrari A. C., Meyer J. C., Scardaci V., Casiraghi C., Lazzeri M., Mauri F., Piscanec S., Jiang D., Novoselov K. S., Roth S., Geim A. K., *Phys. Rev. Lett.* 2006, 97, 187401
- [13]. Kudin K. N., Ozbas B., Schniepp H.C., Prud'homme R. K., Aksay I. A., *Car, Nano Lett.*, 2008, 8, 36
- [14]. Malard L M., Pimenta M A., Dresselhaus G and Dresselhaus M S 2009 Raman spectroscopy in graphene *Phys. Rep.* 473 51.
- [15]. Songfeng P, Hui-Ming C, The reduction of graphene oxide. *Carbon* x x x (2 0 1 1) x x x -x x x
- [16]. Owen C., Bonny J., Dmitriy A., Dikin, Ali A, Khalil A, and SonBinh T. N , Chemically Active Reduced Graphene Oxide with Tunable C/O Ratios, *ACNano*, Vol. 5 ' N. 6 ' 4380-4391 ' 2011
- [17]. Lee C., Wei X., Kysar J. W., Hone J., Measurement of the Elastic Properties and Intrinsic Strength of Monolayer Graphene. *Science* 2008, 321, 385-388
- [18]. Balandin A. A., Ghosh S., Bao W., Calizo I., Teweldebrhan D., Miao, F., Lau C. N., Superior Thermal Conductivity of Single-Layer Graphene. *Nano Lett.* 2008, 8, 902-907.
- [19]. Orlita M., Faugeras C., Plochocka P., Neugebauer P., Martinez G., Maude D. K., Barra A. L., Sprinkle M., Berger C., de Heer W. A., Approaching the Dirac Point in High-Mobility Multilayer Epitaxial Graphene. *Phys. Rev. Lett.* 2008, 101, 267601/1-4.
- [20]. Chen H., Muller M. B., Gilmore K. J., Wallace G. G., Li D., Mechanically Strong, Electrically Conductive, and Biocompatible Graphene Paper. *Adv. Mater.* 2008, 20, 3557-3561.

- [21]. Stankovich S., Dikin D. A., Dommett G. H. B., Kohlhaas K. M., Zimney E. J., Stach E. A., Piner R. D., Nguyen S. T., Ruoff R. S., Graphene-Based Composite Materials. *Nature* 2006, 442, 282–286
- [22]. Fowler J. D., Allen M. J., Tung V. C., Yang Y., Kaner R. B., Weiller B. H., Practical Chemical Sensors from Chemically Derived Graphene. *ACS Nano* 2009, 3, 301–306.
- [23]. Wang C., Li D., Too C. O., Wallace G. G., Electrochemical Properties of Graphene Paper Electrodes Used in Lithium Batteries. *Chem. Mater.* 2009, 21, 2604–2606
- [24]. Abouimrane A., Compton O. C., Amine K., Nguyen S. T., Non-annealed Graphene Paper as a Binder-free Anode for Lithium-Ion Batteries. *J. Phys. Chem. C* 2010, 114, 12800– 12804
- [25]. Park S., An J.H., Jung I. W., Piner R. D., An S. J., Li X. S., Velamakanni A., Ruoff R.S., Colloidal Suspensions of Highly Reduced Graphene Oxide in a Wide Variety of Organic Solvents. *Nano Lett.* 2009, 9, 1593–1597
- [26]. Park S., Ruoff R. S. Chemical Methods for the Production of Graphenes. *Nat. Nanotechnol.* 2009, 4, 217–224.
- [27]. Lerf A., He H., Forster M., Klinowski J., Structure of Graphite Oxide Revisited. *J. Phys. Chem. B* 1998, 102, 4477–4482,
- [28]. Cai W. W., Piner R. D., Stadermann F. J., Park S., Shaibat M. A., Ishii Y., Yang D. X., Velamakanni A., An S. J., Stoller M., Synthesis and Solid-State NMR Structural Characterization of ¹³C-Labeled Graphite Oxide. *Science* 2008, 321, 1815–1817
- [29]. Szabo T., Berkesi O., Forgo P., Josepovits K., Sanakis Y., Petridis D., Dekany I. Evolution of Surface Functional Groups in a Series of Progressively Oxidized Graphite Oxides. *Chem. Mater.* 2006, 18, 2740–2749
- [30]. Compton, O. C., Nguyen S. T., Highly Reduced Graphene Oxide, and Graphene: Versatile Building Blocks for Carbon-Based Materials. *Small* 2010, 6, 711–723

- [31]. Stankovich S., Piner R. D., Nguyen S. T., Ruoff R. S., Synthesis and Exfoliation of Isocyanate-Treated Graphene Oxide Nanoplatelets. *Carbon* 2006, 44, 3342–3347
- [32]. Niyogi S., Bekyarova E., Itkis M. E., McWilliams J. L., Hamon M. A., Haddon R. C., Solution Properties of Graphite and Graphene. *J. Am. Chem. Soc.* 2006, 128, 7720– 7721.
- [33]. Brodie B.C., Sur le poids atomique du graphite. *Ann Chim Phys* 1860;59:466–72.
- [34]. Hummers W., Offeman R., Preparation of graphitic oxide. *J Am Chem Soc* 1958;80:1339.
- [35]. Staudenmaier L. Verfahren zur darstellung der graphitsaure. *Ber Dtsch Chem Ges* 1898;31:1481–99.
- [36]. He H, Riedl T, Lerf A, Klinowski J. Solid-state NMR studies of the structure of graphite oxide. *J Phys Chem* 1996;100(51):19954–8.
- [37]. He H, Klinowski J, Forster M, Lerf A. A new structural model for graphite oxide. *Chem Phys Lett* 1998;287(1,2):53–6.
- [38]. Lerf A, He H, Riedl T, Forster M, Klinowski J. ^{13}C and ^1H MAS NMR studies of graphite oxide and its chemically modified derivatives. *Solid State Ionics* 1997;101–103(Pt. 2):857–62.
- [39]. Lerf A, He H, Forster M, Klinowski J. Structure of graphite oxide revisited. *J Phys Chem B* 1998;102(23):4477–82.
- [40]. Szabo T, Berkesi O, Dekany I. DRIFT study of deuterium-exchanged graphite oxide. *Carbon* 2005;43(15):3186–9.
- [41]. Hontoria-Lucas C., Lopez-Peinado A.J, Lopez-Gonzalez JdD, Rojas-Cervantes ML, Martin-Aranda RM. Study of oxygen-containing groups in a series of graphite oxides: Physical and chemical characterization. *Carbon* 1995;33(11):1585–92.

- [42]. Schniepp H.C, Li J-L, McAllister M.J, Sai H., Herrera-Alonso M, Adamson D.H, Functionalized single graphene sheets derived from splitting graphite oxide. *J Phys Chem B* 2006;110(17):8535–9.
- [43]. Boehm H.P, Clauss A., Fischer G.O., Hofmann U., Thin carbon leaves. *Z Naturforsch* 1962;17b:150–3.
- [44]. Boehm H.P, Clauss A., Fischer G.O, Hofmann U. The adsorption behavior of very thin carbon films. *Z Anorg Allg Chem* 1962;316:119–27.
- [45]. Bourlinos A.B, Gournis D., Petridis D., Szabo T., Szeri A., Dekany I. Chemical reduction to graphite and surface modification with primary aliphatic amines and amino acids. *Langmuir* 2003;19(15):6050–5.
- [46]. Boehm H.P., Clauss A., Fischer G.O., Hofmann U., Thin carbon leaves. *Z Naturforsch* 1962;17b:150–3.
- [47]. Boehm H.P., Clauss A., Fischer G.O., Hofmann U., The adsorption behavior of very thin carbon films. *Z Anorg Allg Chem* 1962;316:119–27
- [48]. Stankovich S., Piner R.D., Chen X., Wu N., Nguyen S.T., Ruoff R.S., Stable aqueous dispersions of graphitic nanoplatelets via the reduction of exfoliated graphite oxide in the presence of poly(sodium 4-styrenesulfonate). *J Mater Chem* 2006;16(2):155–8.
- [49]. Stankovich S., Piner R.D., Nguyen S.T., Ruoff R.S., Synthesis and exfoliation of isocyanate-treated graphene oxide nanoplatelets. *Carbon* 2006;44(15):3342–7.
- [50]. Stankovich S., Dikin D.A, Dommett G.H.B, Kohlhaas K.M, Zimney E.J, Stach E.A, Graphene-based composite materials. *Nature* 2006;442(7100):282–6.
- [51]. Liu Z.B., L. Li., Xu Y.F., and Tian J.G., *J. Optics* 13, 085601 (2011)
- [52]. Sokolov D.E., Shepperd K.R, and Orlando T.M., *J. Phys. Chem. Lett.* 1, 2633 (2010).
- [53]. Zhang Y., Guo L., Wei S., Hei Y., and Sun H., *Nano Today* 5, 15-20 (2010).

[54]. Trusovas R., Raciukaitis G., Barkauskas J. J.of Laser Micro-Nanoengineering, Vol.7, N1, 49-53 (2012).

[55]. Kumar K. S., Subrahmanyam C. N. R., Rao , J. Maters Science, 2012
Graphene produced by radiation-induced reduction of graphene oxide.



4.9 CONCLUSION

The first objective of this thesis was to synthesize, characterize and investigate various properties of graphene or reduced graphene oxide. More specifically graphene oxide and reduced graphene oxide solutions prepared by Hummers method have been deposited on silicon substrates separately. Several techniques have been employed to characterize GO and RGO deposited on silicon substrates with the aim of investigating different properties of GO and rGO.

Hummers method is a cost efficient production method due to the price of raw materials but chemical processing completely introduces defects in the course of oxidation or reduction and functionalization in reduced graphene oxide sheets resulting to the decrease in conductivity [1] Thus the main challenge for accumulation of this process is to acquire routes for complete reformation of the sp^2 carbon network of reduced graphene oxide.

ATR-FTIR revealed the presence of OFG before reduction, after reduction the very same technique confirms fewer OFG in the reduced graphene oxide, this was further confirmed by the UV-Vis result when 225 nm absorption peak appeared after oxidation of graphite to graphene, the same peak shifted to 280 nm after reduction of graphene oxide to reduced graphene oxide. The 280 nm peak confirmed that most excess of oxygen functional groups have been removed. According to reference [2], the displaced peaks are due to the $\pi \rightarrow \pi^*$ transition for the C=C bonding.

The characterized films of GO and rGO exhibited the presence of OFG in AFM, results showed that GO has a lot of oxygen functional groups, this was

proved by the measured roughness of both GO and rGO. GO has a higher roughness than rGO which means there are more oxygen functional groups in GO which are stacked together than in rGO.

SEM showed some rippling and folding of stacked GO sheets before reduction, after reduction it showed wrinkled structure with less oxygen functional groups. TEM showed flake-like tightly packed GO sheets before reduction, after the reduction process the rGO sheets were stacked on top of one another to form a film. Raman spectrum showed D and G bands for both GO and rGO sheets but for rGO there is G* and 2D bands which are associated with the reduction process of GO to rGO.

All and all, the used techniques are in agreement, all displaced the expected information about graphene oxide and reduced graphene oxide.

The second objective of this project was to reduce GO using the sun and artificial light, more specifically GO solutions were exposed to sunlight for 2h , 4h, 8h, 16h and 32h. After 2h of irradiation the color changed from brownish yellow to black. The other durations also confirmed the color change. After irradiating GO for the above durations, three characterization techniques (XRD, ATR-FTIR and UV-VIS-NIR) were used to further confirm the reduction of GO. The obtained results were complementary to the previous results of *Rao et al* [3].

In the case of reducing GO using filtered artificial light, five lamps i.e green, blue, yellow, red and white were used to irradiate GO. GO solutions were exposed to each filtered artificial light as shown in figure 4.12 . Each solution was exposed for 2h, 4h, 8h and 16h. The XRD, ATR-FTIR and UV-VIS

confirmed the reduction of GO. One can conclude that indeed using the sun and artificial light, we can produce graphene.



4.10 References

- [1]. Zhang, Y.B. et al. (2005) Experimental observation of the quantum Hall effect and Berry's phase in graphene. *Nature* 438, 201–204
- [2]. Mei Q, Zhang K, Guan G, Liu B, Wang S, Zhang Z. Highly efficient photoluminescent graphene oxide with tunable surface properties. *Chem Commun.* 2010;46:7319–7321.
- [3]. Graphene produced by radiation-induced reduction of graphene oxide
Prashant Kumar, K. S. Subrahmanyam, C. N. R. Rao , J. Mater Science, 2012



4.11 APPENDICES

4.11.1 APPENDIX A

Lattice structure	Hexagonal
Lattice constant (Å)	2.462
Atomic density (C atomic/ cm ³)	1.14×10^{23}
Specific gravity (g / cm ³)	2.26
Specific heat (cal/ g. K)	0.17
Thermal conductivity (W/ cm.K)	30
Binding energy (eV/ C atom)	7.4
Debye temperature (K)	2500 950
Bulk modulus (GPa)	1060 36.5
Band gap (eV)	-0.04
Carrier density (10^{18} /cm ² at 4K	5
Electron mobility (cm ² / V sec)	20,000 100
Hole mobility (cm ² /V sec)	15,000 90

Resistivity (Ωcm)	50×10^{-6}
Melting point (K)	4450

Appendix A: Properties of Graphite [13]

4.11.2 **APPENDIX B**

Lattice structure	Cubic
Lattice constant (Å)	3.567
Atomic density (C atoms/cm ³)	1.77×10^{23}
Specific gravity (C atoms/cm ³)	3.515
Specific heat (cal/g.K)	0.12
Thermal conductivity (W/cm. K)	~25
Binding energy (eV/ C atom)	7.2
Debye temperature (K)	1860
Bulk modulus (GPa)	42.2

Band gap (eV)	10
Carrier density ($10^{18}/\text{cm}^3$ at 4K)	0
Electron mobility ($\text{cm}^2/\text{V sec}$)	1800
Hole mobility (cm^2/Vsec)	1500
Melting point (K)	4500

Appendix B: Shows the summary of various properties of diamond [13]

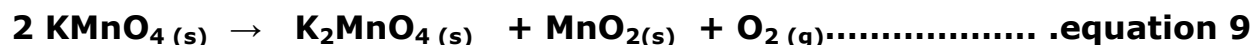


4.11.3 APPENDIX C

Hummers method uses chemicals and acids, below is the brief discussion of the chemicals and acids used for preparation.

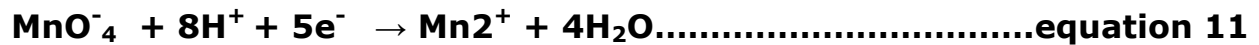
POTASSIUM PERMANGANATE (KMnO_4)

Potassium permanganate is an inorganic chemical compound with the formula KMnO_4 . It is a salt of K^+ and MnO_4^- ions. Formerly known as permanganate potash, it is a strong oxidation agent. Potassium permanganate decomposes when exposed to light:



Potassium permanganate is able to oxidize primary alcohols to carboxylic acids

Under acidic conditions the oxidation half-reactions are:



Under alkaline conditions, the half-reaction is



Reaction rates for the oxidation of constituents found in natural waters are relatively fast and depend on temperature, pH and dosage

SULPHURIC ACID (H₂SO₄)

Sulfuric acid is a clear, colorless, viscous liquid that is very corrosive.

Sulfuric acid is often prepared as a byproduct from mining operations. Many metals ores are sulfides and smelting operations eliminate sulfur in the form of sulphuric dioxide gas. The sulphuric dioxide gas is cleaned and converted into sulphuric acid.



Sulphuric acid is used as a drying agent to chemically remove water from my substances.

HYDROGEN PEROXIDE (H₂O₂)

A mixture of H₂SO₄ and H₂O₂ is used to clean organic residues off substrates. Because the mixture is a strong oxide, it will remove most organic matter, and it will also hydroxylate most surfaces (add -OH groups), making them extremely hydrophilic (water compatible).



HYDROCHLORIC ACID (HCl)

Hydrogen Chloride (HCl) is a monoprotic acid, which means it can dissociate (ionize) only once to give up one H⁺ ion (a single proton). In aqueous Hydrochloric acid, the H⁺ joins water molecule to form a hydronium ion H₃O⁺.



Since Hydrochloric acid is a strong acid, it is completely dissociated in water.

HYDRAZINE HYDRATE (N₂H₄)

Hydrazine is an inorganic compound with the formula N₂H₄. It is a colorless flammable liquid with an ammonia-like odor. Hydrazine is highly toxic and dangerously unstable unless handled in solution.

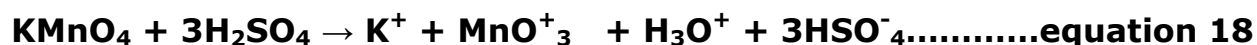
Hydrazine has basic (alkali) chemical properties comparable to ammonia:



Hydrazine is a convenient reductant because the by-products are typically nitrogen gas and water thus; it is used as an antioxidant, an oxygen scavenger, and a corrosion inhibitor in water boilers and heating systems. It is also used to reduce salts and oxides to the pure metals in electrolysis nickel plating and plutonium extraction from nuclear reactor waste.

OXIDATION.

The purpose of adding H₂SO₄ in a solution is to increase the acidity of the solution and reacting acid with permanganate is to create MnO₄⁻ that reacts with Mn²⁺ to produce Mn₂O₇ as shown by the chemical reactions below.



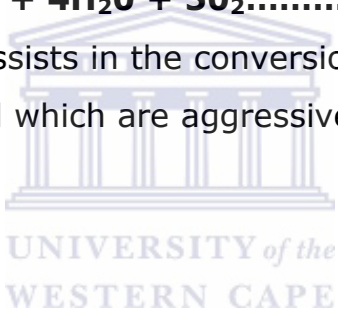


The formation of dimanganese heptoxide (Mn_2O_7) from KMnO_4 in the presence of strong acid is desirable since Mn_2O_7 is a strong oxidizing agent which is needed to oxidize graphite to graphite oxide.

By slowly adding potassium permanganate, the MnO^+_3 ion reacts with the MnO^-_4 resulting in dimanganese heptoxide Mn_2O_7 which is a strong oxidizing agent, hence the reduction of graphite to graphite oxide.



Again, Sulphuric acid also assists in the conversion of hydrogen peroxide into hydronium ion and O radical which are aggressive oxidant



REDUCTION.

The hydrazine hydrate dissociates in water to create a hydroxyl ion that reacts with oxygen in the graphitic structure after exfoliation process that resulted from oxidation to reduce graphene oxide to reduce graphene oxide . And the metal ions that are Mn^{2+} and K^+ will react with chlorine ion and the H^+ will react with the OH^- from hydrazine as follows.





UNIVERSITY *of the*
WESTERN CAPE